



ChemComm

**Axially chiral 1,1'-bicarbazolyls with near-ultraviolet circularly polarized luminescence**

Journal:	<i>ChemComm</i>
Manuscript ID	CC-COM-02-2022-000936.R1
Article Type:	Communication

SCHOLARONE™  
Manuscripts

## COMMUNICATION

## Axially chiral 1,1'-bicarbazolyls with near-ultraviolet circularly polarized luminescence

So Shikita,<sup>ab</sup> Takunori Harada<sup>c</sup> and Takuma Yasuda<sup>\*ab</sup>Received 00th January 20xx,  
Accepted 00th January 20xx

DOI: 10.1039/x0xx00000x

The facile synthesis and chiroptical properties of a new family of circularly polarized luminescence (CPL) materials, axially chiral 1,1'-bicarbazolyls (BiCz), is reported. The BiCz derivatives emitted intense near-ultraviolet photoluminescence, with a peak at ~380 nm. The BiCz enantiomers showed mirror-image circular dichroism and CPL, with  $g_{lum}$  values on the order of  $10^{-4}$  in solution.

Axially chiral biaryls, typified by 1,1'-binaphthyl derivatives, are indispensable stereogenic motifs for chiral ligands and chiral organocatalysts in asymmetric synthesis.<sup>1,2</sup> Apart from their use in organic synthesis, the development of axially chiral biaryls as chiroptical functional  $\pi$ -materials<sup>3</sup> with circularly polarized luminescence (CPL) properties has gained increasing interest.<sup>4</sup> The interest in CPL materials stems from their prospective applications in 3D displays,<sup>5</sup> optical quantum information<sup>6</sup> and security systems,<sup>7</sup> biological probes/sensors,<sup>8</sup> and the control of plant growth. The use of axially chiral 1,1'-binaphthyl has enabled the development of a variety of CPL-active materials, including organic fluorophores,<sup>4a,i,j,9,10</sup> thermally activated delayed fluorescence (TADF) emitters,<sup>4b,c,5b,11</sup> and metal complex phosphors.<sup>12</sup> However, the structural variety and functional extensibility are relatively low because they rely on the conventional 1,1'-binaphthyl scaffold.

Carbazole is among the most widely used  $\pi$ -conjugated building unit, finding prominent utility in optoelectronic device applications including organic light-emitting diodes (OLEDs).<sup>13</sup> This widespread use prompted us to design a novel, functional axially chiral motif featuring carbazole. However, the reports on carbazole-based CPL materials are still scarce.<sup>14</sup> It is well known that carbazole are readily functionalized by electrophilic aromatic substitution at the 3,6-positions (*para* positions from

the nitrogen atom) with high electron densities. Therefore, further functionalization of the carbazole at the 1,8-positions (*ortho* positions from the nitrogen atom) can proceed by protecting the most reactive 3,6-positions. The 3,6-disubstituted 1,1'-bicarbazolyl (BiCz-H) framework can be constructed by Ni(0)-mediated dehalogenative coupling (Yamamoto coupling) or oxidative coupling.<sup>15</sup> To produce left- and right-handed CPL, the (*R*)- and (*S*)-enantiomeric forms of the chiral substance must be prepared. However, isolating the non-racemic (enantiomeric) forms of BiCz-H is impossible because the aryl-aryl bond is not sterically congested (Fig. 1a). Therefore, further *N*-arylation of BiCz-H is exploited herein to induce a large rotational barrier to yield a resolvable 1,1'-bicarbazolyl-based chiral  $\pi$ -system. The simplicity and versatility of this post-*N*-functionalization enable further exploration of the potential of 1,1'-bicarbazolyl derivatives as CPL materials. Herein, we report the facile synthesis of axially chiral 1,1'-bicarbazolyls, BiCz-1 and BiCz-2 (Fig. 1b), and their fundamental photophysical and chiroptical properties.

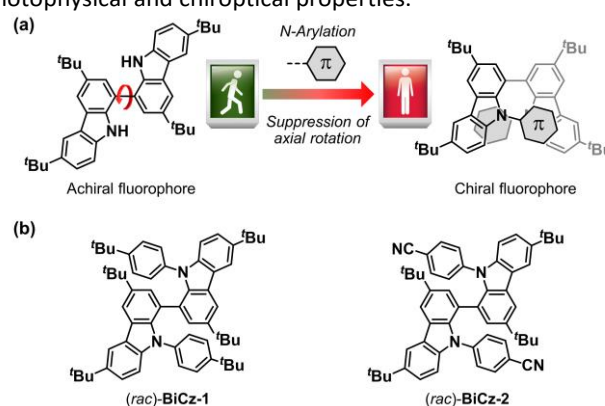


Fig. 1 (a) Design of novel axially chiral 1,1'-bicarbazolyls and (b) chemical structures of BiCz-1 and BiCz-2.

Scheme 1 outlines the facile two-step synthesis of the racemic 1,1'-bicarbazolyls, (*rac*)-BiCz-1 and (*rac*)-BiCz-2, from commercially available 3,6-di(*tert*-butyl)carbazole. Cu(ClO<sub>4</sub>)<sub>2</sub> was used for the direct oxidative coupling of 3,6-di(*tert*-butyl)carbazole under the optimized conditions to furnish

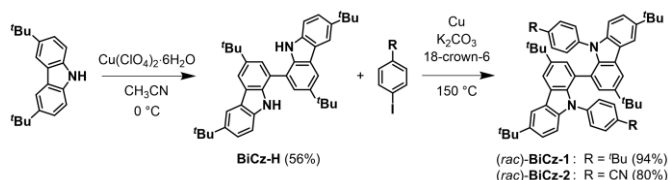
<sup>a</sup> INAMORI Frontier Research Center (IFRC), Kyushu University, 744 Motoooka, Nishi-ku, Fukuoka 819-0395, Japan. E-mail: yasuda@ifrc.kyushu-u.ac.jp

<sup>b</sup> Department of Applied Chemistry, Graduate School of Engineering, Kyushu University, 744 Motoooka, Nishi-ku, Fukuoka 819-0395, Japan

<sup>c</sup> Department of Integrated Science and Technology, Faculty of Science and Technology, Oita University, 700 Dannoharu, Oita 870-1192, Japan

†Electronic Supplementary Information (ESI) available: Experimental procedures, additional data and spectra. CCDC 2151609. See DOI: 10.1039/x0xx00000x

dimeric **BiCz-H** in 56% yield. Subsequently, **BiCz-H** was subjected to Ullmann coupling with 1-(*tert*-butyl)-4-iodobenzene and 4-iodobenzonitrile to afford (*rac*)-**BiCz-1** and (*rac*)-**BiCz-2** in 94% and 80% yields, respectively. The chemical structures of these products were confirmed by  $^1\text{H}$  and  $^{13}\text{C}$  NMR spectroscopy, mass spectrometry, and elemental analysis (ESI $^+$ ). Successive optical resolutions were achieved using preparative HPLC on a chiral stationary phase, affording sufficient of both enantiomers of **BiCz-1** and **BiCz-2** in >99% enantiomeric excess (e.e.). The absolute configurations for the first fractions of **BiCz-1** and **BiCz-2** in the chiral HPLC analyses could be determined as (*S*)-**BiCz-1** and (*S*)-**BiCz-2**, respectively, by comparison of the experimental circular dichroism (CD) spectra and computational simulation results (ESI $^+$ ). The *N*-aryl groups effectively suppressed racemization of both enantiomers, allowing them to retain stable axial chirality, unlike unsubstituted **BiCz-H**. Both resolved (*S*)-**BiCz-1** and (*S*)-**BiCz-2** were found to retain >99% e.e. in toluene solution even when kept for 1 day at room temperature. However, upon heating the solutions at 100 °C for 1 h, the e.e. decreased to 95% and 90%, respectively (ESI $^+$ ).



Scheme 1 Synthesis of axially chiral 1,1'-bicarbazolyl derivatives.

X-ray crystallographic analysis revealed that (*rac*)-**BiCz-1** crystallized in the orthorhombic *Pbca* space group (Fig. 2 and ESI $^+$ ). In a single crystal of (*rac*)-**BiCz-1**, there are eight molecules per unit cell, comprising four of each (*R*)- and (*S*)-enantiomer with mirror symmetry. The dihedral angles of the central 1,1'-bicarbazolyl units are all approximately  $\pm 60^\circ$ , suggestive of large steric hindrance around the chiral axis.

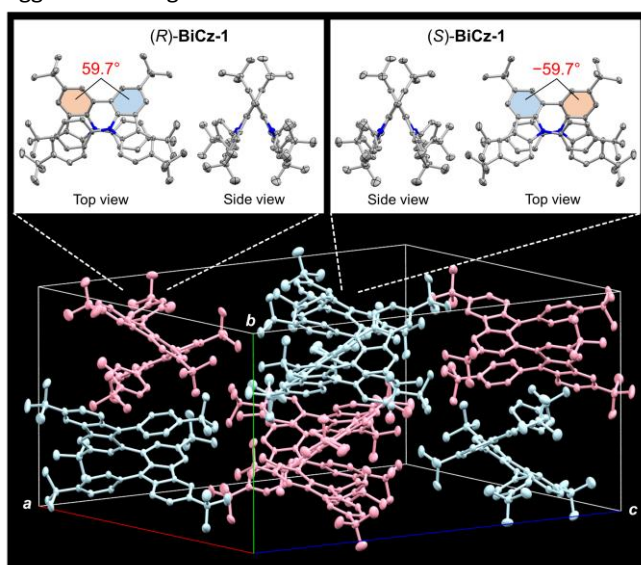


Fig. 2 X-ray crystal structure of (*rac*)-**BiCz-1** (CCDC No. 2151609): (top) ORTEP drawings of (*R*)-**BiCz-1** (left) and (*S*)-**BiCz-1** (right) enantiomers with thermal ellipsoids at the 50% probability level; (bottom) molecular packing diagram containing equimolar (*R*)- and (*S*)-enantiomers (pink and light-blue molecules, respectively). Hydrogen atoms and solvent molecules ( $\text{CHCl}_3$ ) are omitted for clarity.

To gain insight into the molecular geometries and electronic transition characteristics, density functional theory (DFT) and time-dependent DFT (TD-DFT) calculations were performed for **BiCz-1** and **BiCz-2** at the B3LYP-D3/6-31G(d) level (Fig. 3).<sup>16</sup> In **BiCz-1** and **BiCz-2**, the 1,1'-bicarbazolyl units adopted a highly twisted geometry around the chiral axis in the ground state ( $S_0$ ), with dihedral angles were  $58.8^\circ$  and  $54.9^\circ$ , respectively. This result is consistent with the aforementioned crystallographic data. For 4-*tert*-butylphenyl-substituted **BiCz-1**, the lowest singlet ( $S_1$ ) excitation was dominated by the HOMO  $\rightarrow$  LUMO transition with  $\pi$ - $\pi^*$  characteristics. Contrastingly, in 4-cyanophenyl-substituted **BiCz-2**, the  $S_1$  excitation was characterized by a forbidden HOMO  $\rightarrow$  LUMO transition with intramolecular charge transfer (ICT) characteristics. In this transition, the HOMO was distributed over the entire molecule, whereas the LUMO was mainly localized on the electron-accepting 4-cyanophenyl groups. The intensive electronic excitations corresponded to the allowed HOMO-1  $\rightarrow$  LUMO ICT transition ( $S_4$ ) and HOMO  $\rightarrow$  LUMO+2  $\pi$ - $\pi^*$  transition ( $S_5$ ), with relatively large oscillator strengths ( $f = 0.1844$  and  $0.0754$ , respectively).

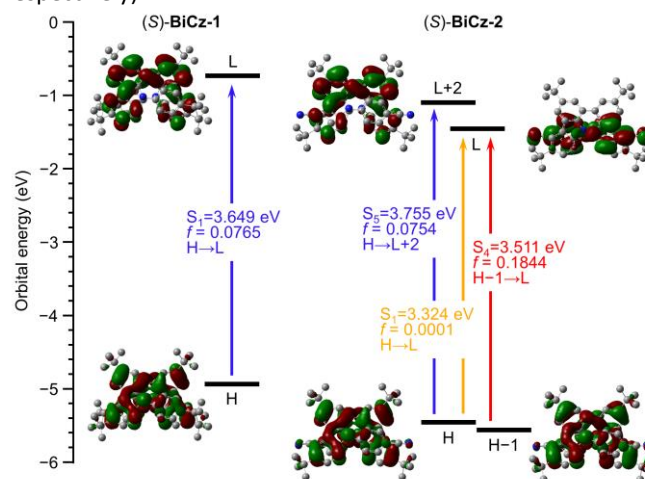
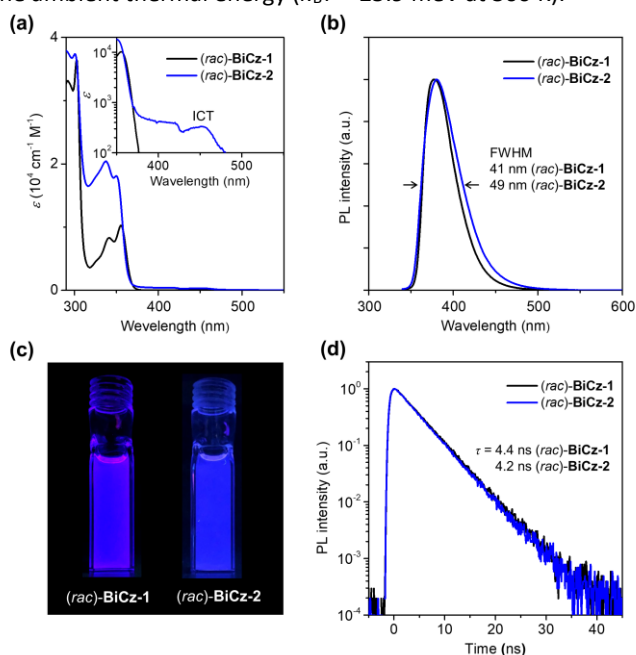


Fig. 3 Electronic transition and associated Kohn-Sham orbitals for (*S*)-**BiCz-1** (left) and (*S*)-**BiCz-2** (right) in optimized  $S_0$  geometries, calculated at the B3LYP-D3/6-31G(d) level in the gas phase. H = HOMO; L = LUMO.

Fig. 4 shows the photophysical spectroscopic properties of (*rac*)-**BiCz-1** and (*rac*)-**BiCz-2** in toluene, including the UV-vis absorption and photoluminescence (PL) spectra and transient PL curves. The lowest-energy absorption band of (*rac*)-**BiCz-1** was observed at 355 nm, and was assigned to the  $\pi$ - $\pi^*$  transition. (*rac*)-**BiCz-1** also emitted intense near-ultraviolet (NUV) photoluminescence (PL) with a peak ( $\lambda_{\text{PL}}$ ) at 377 nm; the absolute PL quantum yield ( $\Phi_{\text{PL}}$ ) was as high as 94%. Notably, the spectral full width at half maximum (FWHM) of (*rac*)-**BiCz-1** was as small as 41 nm, which reflects its rigid molecular structure. As predicted by the TD-DFT calculations (Fig. 3), a very weak ICT absorption centered at 450 nm was observed for (*rac*)-**BiCz-2**. However, the PL of (*rac*)-**BiCz-2** predominantly occurred in the NUV region ( $\lambda_{\text{PL}} = 383$  nm), similar to (*rac*)-**BiCz-1** (Fig. 4b,c). The  $\Phi_{\text{PL}}$  of (*rac*)-**BiCz-2** (44%) was less than half that of (*rac*)-**BiCz-1**, most likely because of deactivation through non-radiative internal conversion and/or intersystem crossing. The transient PL characteristics of both compounds had similar monoexponential emission decays with lifetimes ( $\tau$ ) of 4.2–4.4

ns at 300 K (Fig. 4d), indicative of typical fluorescence properties. Based on these photophysical data, the fluorescence radiative decay rate ( $k_r = \Phi_{PL}/\tau$ ) and the non-radiative decay rate ( $k_{nr} = (1 - \Phi_{PL})/\tau$ ) can be assessed. Both (*rac*)-**BiCz-1** and (*rac*)-**BiCz-2** had comparably high  $k_r$  values of  $2.1 \times 10^8$  and  $1.0 \times 10^8$  s<sup>-1</sup>, respectively; however, the  $k_{nr}$  of (*rac*)-**BiCz-2** ( $1.3 \times 10^8$  s<sup>-1</sup>) was one order of magnitude larger than that of (*rac*)-**BiCz-1** ( $1.4 \times 10^7$  s<sup>-1</sup>). Moreover, no distinct TADF properties were observed for either compound because of their considerably large singlet–triplet energy gap ( $\Delta E_{ST} > 0.5$  eV; ESIT<sup>+</sup>) with respect to the ambient thermal energy ( $k_B T \approx 25.9$  meV at 300 K).



**Fig. 4** (a) UV–vis absorption and (b) steady-state PL spectra of (*rac*)-**BiCz-1** and (*rac*)-**BiCz-2** in deoxygenated toluene solutions ( $10^{-5}$  M). The inset of (a) shows a magnified view of the lower-energy ICT absorption. (c) Photograph showing NUV emissions from the solutions under UV illumination at 365 nm. (d) Transient PL decay curves measured for the solutions at 300 K.

Circular dichroism (CD) and CPL spectra were acquired to examine the chiroptical properties of the (*R/S*)-**BiCz-1** and (*R/S*)-**BiCz-2** enantiomer pairs in toluene for the ground and excited states. As shown in Fig. 5a, the CD spectra of the enantiomers exhibited clear mirror-image relationships with strong Cotton effects at 355 nm and absorption dissymmetry factors ( $|g_{abs}|$ ) of  $2 \times 10^{-3}$  (ESIT<sup>+</sup>), which correspond to the  $\pi$ – $\pi^*$  absorption on the chiral 1,1'-bicarbazolyl skeleton. However, (*R/S*)-**BiCz-2** had no significant Cotton effect in the ICT absorption region. The CPL spectra of the (*R/S*)-**BiCz-1** and (*R/S*)-**BiCz-2** solutions showed mirror-image CPL signals (Fig. 5a) with PL dissymmetry factors ( $|g_{lum}|$ ) of  $4 \times 10^{-4}$  and  $6 \times 10^{-4}$ , respectively, at the  $\lambda_{PL}$  positions (Fig. 5b). Although the obtained  $|g_{lum}|$  values are within the normal range for reported CPL materials made from axially chiral biaryls, the luminescence efficiencies can be greatly improved by using the 1,1'-bicarbazolyl  $\pi$ -core instead.

In theory,  $g_{lum}$  is determined as follows:<sup>17</sup>

$$g_{lum} = \frac{2(I_L - I_R)}{(I_L + I_R)} = \frac{4|\mu||m| \cos \theta}{|\mu|^2 + |m|^2} \quad (1)$$

where  $I_L$  and  $I_R$  are the intensities of the left- and right-handed CPL emissions,  $\mu$  and  $m$  are the electric and magnetic transition dipole moments, respectively, and  $\theta$  represents the angle between the  $\mu$  and  $m$  vectors. Complete left- and right-handed

CPL lights lead to the maximum  $g_{lum}$  values of +2 and –2, respectively. Using TD-DFT calculations,  $|\mu|$ ,  $|m|$ , and  $\theta$  for **BiCz-1** and **BiCz-2** were simulated,<sup>16</sup> considering their dominant  $\pi$ – $\pi^*$  and ICT transitions, respectively (ESIT<sup>+</sup>). Consequently, **BiCz-2** exhibited a slightly larger theoretical dissymmetry factor ( $|g_{cal}| = 2.7 \times 10^{-3}$ ) than **BiCz-1** ( $|g_{cal}| = 1.7 \times 10^{-3}$ ), which is reasonably consistent with the trend of the experimental  $|g_{lum}|$  values. In the optimized **BiCz-1** and **BiCz-2** molecules, the  $\mu$  and  $m$  vectors had nearly perpendicular orientations (ESIT<sup>+</sup>), resulting in a small  $|\cos \theta|$  (0.09 and 0.23, respectively) and small  $|g_{lum}|$  on the order of  $10^{-4}$ .

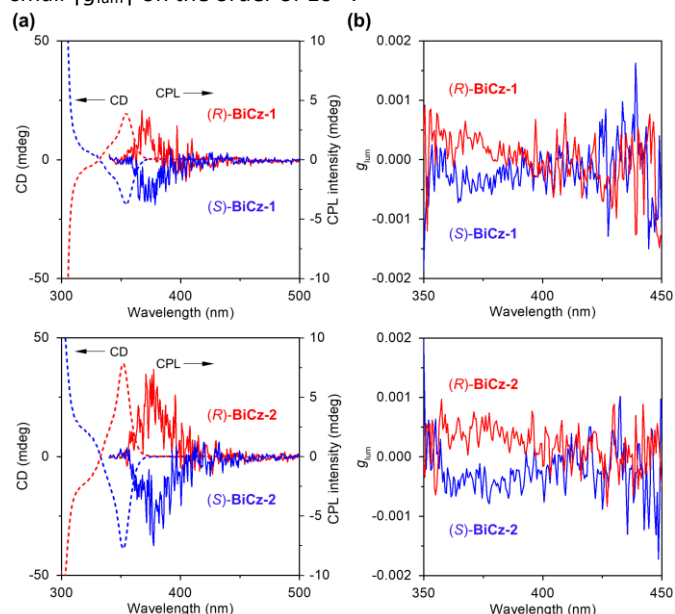


**Fig. 5** (a) CD (dashed lines) and CPL (solid lines) spectra and (b) corresponding  $g_{lum}$  vs. wavelength curves of enantiopure (*R/S*)-**BiCz-1** (upper) and (*R/S*)-**BiCz-2** (lower) in toluene solutions ( $10^{-4}$  M).

In summary, the first axially chiral 1,1'-bicarbazolyl derivatives, (*R/S*)-**BiCz-1** and (*R/S*)-**BiCz-2**, were successfully developed. These materials can be readily synthesized in two steps with high yields. These pairs of enantiomers can emit highly efficient PL in the NUV region, with distinct CPL activity in solution. This study is expected to stimulate the exploration of functional  $\pi$ -materials based on axially chiral 1,1'-bicarbazolyls for chiroptical applications. Further study on material design to enhance the dissymmetry factor is currently underway.

This work was supported in part by Grants-in-Aid for JSPS KAKENHI (Grant No. JP21H04694, JP18H02048) and JST CREST (Grant No. JPMJCR2105). We are grateful for the support provided by the Cooperative Research Program of the “Network Joint Research Center for Materials and Devices” and the computer facilities at the Research Institute for Information Technology, Kyushu University.

## Conflicts of interest

There are no conflicts to declare.

## References and notes

- For reviews, see: (a) R. Noyori, *Angew. Chem. Int. Ed.*, 2002, **41**, 2008; (b) R. Noyori and H. Takaya, *Acc. Chem. Res.*, 1990,

- 23**, 345; (c) Y. Chen, S. Yekta and A. K. Yudin, *Chem. Rev.*, 2003, **103**, 3155; (d) P. Kočovský, Š. Vyskočil and M. Smrčina, *Chem. Rev.*, 2003, **103**, 3213; (e) T. Akiyama, *Chem. Rev.*, 2007, **107**, 5744; (f) D. Parmar, E. Sugiono, S. Raja and M. Rueping, *Chem. Rev.*, 2014, **114**, 9047.
- 2 (a) A. Miyashita, A. Yasuda, H. Takaya, K. Toriumi, T. Ito, T. Souchi and R. Noyori, *J. Am. Chem. Soc.*, 1980, **27**, 7932; (b) T. Ooi, M. Kameda and K. Maruoka, *J. Am. Chem. Soc.*, 1999, **121**, 6519; (c) T. Akiyama, J. Itoh, K. Yokota and K. Fuchibe, *Angew. Chem. Int. Ed.*, 2004, **43**, 1566; (d) D. Uraguchi and M. Terada, *J. Am. Chem. Soc.*, 2004, **126**, 5356.
- 3 (a) G. Albano, G. Pescitelli and L. D. Bari, *Chem. Rev.*, 2020, **120**, 10145; (b) J. R. Brandt, F. Salerno and M. J. Fuchter, *Nat. Rev. Chem.*, 2017, **1**, 0045.
- 4 For reviews, see: (a) L. Arrico, L. D. Bari and F. Zinna, *Chem. Eur. J.*, 2021, **27**, 2920; (b) L. Frédéric, A. Desmarchelier, L. Favereau, G. Pieters, *Adv. Funct. Mater.*, 2021, **31**, 2010281; (c) X. Li, Y. Xie and Z. Li, *Adv. Photonics Res.*, 2020, **2**, 2000136; (d) T. Zhao, J. Han, P. Duan and M. Liu, *Acc. Chem. Res.*, 2020, **53**, 1279; (e) A. Nitti and D. Pasini, *Adv. Mater.*, 2020, **32**, 1908021; (f) Y. Sang, J. Han, T. Zhao, P. Duan and M. Liu, *Adv. Mater.*, 2020, **32**, 1900110; (g) F. Song, Z. Zhao, Z. Liu, J. W. Y. Lam and B. Z. Tang, *J. Mater. Chem. C*, 2020, **8**, 3284; (h) J.-L. Ma, Q. Peng and C.-H. Zhao, *Chem. Eur. J.*, 2019, **25**, 15441; (i) H. Tanaka, Y. Inoue and T. Mori, *ChemPhotoChem*, 2018, **2**, 386; (j) J. Han, S. Guo, H. Lu, S. Liu, Q. Zhao and W. Huang, *Adv. Optical Mater.*, 2018, **6**, 1800538; (k) E. M. Sánchez-Carnerero, A. R. Agarrabeitia, F. Moreno, B. L. Maroto, G. Muller, M. J. Ortiz and S. de la Moya, *Chem. Eur. J.*, 2015, **21**, 13488; (l) J. Kumar, T. Nakashima and T. Kawai, *J. Phys. Chem. Lett.*, 2015, **6**, 3445.
- 5 (a) D.-W. Zhang, M. Li and C.-F. Chen, *Chem. Soc. Rev.*, 2020, **49**, 1331; (b) L. Zhou, G. Xie, F. Ni and C. Yang, *Appl. Phys. Lett.*, 2020, **117**, 130502; (c) D.-Y. Kim, *J. Korean Phys. Soc.*, 2006, **49**, 505.
- 6 Y. Yang, R. C. da Costa, M. J. Fuchter and A. J. Campbell, *Nat. Photonics*, 2013, **7**, 634.
- 7 L. E. MacKenzie and R. Pal, *Nat. Rev. Chem.*, 2021, **5**, 109.
- 8 (a) M. C. Heffern, L. M. Matosziuk and T. J. Meade, *Chem. Rev.*, 2014, **114**, 4496; (b) X. Zhang, J. Yin and J. Yoon, *Chem. Rev.*, 2014, **114**, 4918.
- 9 (a) Y. Imai, *Chem. Lett.*, 2021, **50**, 1131; (b) T. Kimoto, N. Tajima, M. Fujiki and Y. Imai, *Chem. Asian J.*, 2012, **7**, 2836; (c) T. Kinuta, N. Tajima, M. Fujiki, M. Miyazawa and Y. Imai, *Tetrahedron*, 2012, **68**, 4791; (d) T. Amako, T. Harada, N. Suzuki, K. Mishima, M. Fujiki and Y. Imai, *RSC Adv.*, 2013, **3**, 23508; (e) S. Nakanishi, K. Nakabayashi, T. Mizusawa, N. Suzuki, S. Guo, M. Fujiki and Y. Imai, *RSC Adv.*, 2016, **6**, 99172; (f) D. Kaji, S. Ikeda, K. Takamura, N. Tajima, M. Shizuma, T. Mori, M. Miyasaka and Y. Imai, *Chem. Lett.*, 2019, **48**, 874.
- 10 (a) T. Kawai, K. Kawamura, H. Tsumatori, M. Ishikawa, M. Naito, M. Fujiki and T. Nakashima, *ChemPhysChem*, 2007, **8**, 1465; (b) H. Maeda, Y. Bando, K. Shimomura, I. Yamada, M. Naito, K. Nobusawa, H. Tsumatori and T. Kawai, *J. Am. Chem. Soc.*, 2011, **133**, 9266; (c) J. Kumar, T. Nakashima, H. Tsumatori and T. Kawai, *J. Phys. Chem. Lett.*, 2014, **5**, 316; (d) E. M. Sánchez-Carnerero, F. Moreno, B. L. Maroto, A. R. Agarrabeitia, M. J. Ortiz, B. G. Vo, G. Muller and S. de la Moya, *J. Am. Chem. Soc.*, 2014, **136**, 3346; (e) K. Hassan, K. Yamashita, K. Hirabayashi, T. Shimizu, K. Nakabayashi, Y. Imai, T. Matsumoto, A. Yamano and K. Sugiura, *Chem. Lett.*, 2015, **44**, 1607; (f) S. Hirata and M. Vacha, *J. Phys. Chem. Lett.*, 2016, **7**, 1539; (g) K. Takaishi, T. Yamamoto, S. Hinoide and T. Ema, *Chem. Eur. J.*, 2017, **23**, 9249; (h) K. Takaishi, R. Takehana and T. Ema, *Chem. Commun.*, 2018, **54**, 1449; (i) X. Zhang, Y. Zhang, Y. Li, Y. Quan, Y. Cheng and Y. Li, *Chem. Commun.*, 2019, **55**, 9845; (j) X. Zhang, Y. Zhang, H. Zhang, Y. Quan, Y. Li, Y. Cheng and S. Ye, *Org. Lett.*, 2019, **21**, 439; (k) Z.-B. Sun, J.-K. Liu, D.-F. Yuan, Z.-H. Zhao, X.-Z. Zhu, D.-H. Liu, Q. Peng and C.-H. Zhao, *Angew. Chem. Int. Ed.*, 2019, **58**, 4840; (l) K. Takaishi, K. Iwachido and T. Ema, *J. Am. Chem. Soc.*, 2020, **142**, 1774; (m) X. Wu, C.-Y. Huang, D.-G. Chen, D. Liu, C. Wu, K.-J. Chou, B. Zhang, Y. Wang, Y. Liu, E. Y. Li, W. Zhu and P.-T. Chou, *Nat. Commun.*, 2020, **11**, 2145.
- 11 (a) S. Feuillastre, M. Pauton, L. Gao, A. Desmarchelier, A. J. Riives, D. Prim, D. Tondelier, B. Geffroy, G. Muller, G. Clavier and G. Pieters, *J. Am. Chem. Soc.*, 2016, **138**, 3990; (b) F. Song, Q. Zhang, Z. Zhao, H. Zhang, W. Zhao, Z. Qiu, C. Qi, H. Zhang, H. H. Y. Sung, I. D. Williams, J. W. Y. Lam, Z. Zhao, A. Qin, D. Ma and B. Z. Tang, *Adv. Funct. Mater.*, 2018, **28**, 1800051; (c) Z.-G. Wu, H.-B. Han, Z.-P. Yan, X.-F. Luo, Y. Wang, Y.-X. Zheng, J.-L. Zuo and Y. Pan, *Adv. Mater.*, 2019, **31**, 1900524; (d) Z.-G. Wu, Z.-P. Yan, X.-F. Luo, L. Yuan, W.-Q. Liang, Y. Wang, Y.-X. Zheng, J.-L. Zuo and Y. Pan, *J. Mater. Chem. C*, 2019, **7**, 7045; (e) S. Sun, J. Wang, L. Chen, R. Chen, J. Jin, C. Chen, S. Chen, G. Xie, C. Zheng and W. Huang, *J. Mater. Chem. C*, 2019, **7**, 14511; (f) Y. Wang, Y. Zhang, W. Hu, Y. Quan, Y. Li and Y. Cheng, *ACS Appl. Mater. Interfaces*, 2019, **11**, 26165; (g) L. Frédéric, A. Desmarchelier, R. Plais, L. Lavnech, G. Muller, C. Villafuerte, G. Clavier, E. Quesnel, B. Racine, S. Meunier-Della-Gatta, J.-P. Dognon, P. Thuéry, J. Grassous, L. Favereau and G. Pieters, *Adv. Funct. Mater.*, 2020, **30**, 2004838.
- 12 (a) T. Harada, Y. Nakano, M. Fujiki, M. Naito, T. Kawai and Y. Hasegawa, *Inorg. Chem.*, 2009, **48**, 11242; (b) J. Song, M. Wang, X. Zhou and H. Xiang, *Chem. Eur. J.*, 2018, **24**, 7128; (c) J. Song, M. Wang, X. Xu, L. Qu, X. Zhou and H. Xiang, *Dalton Trans.*, 2019, **48**, 4420; (d) J. Han, S. Guo, J. Wang, L. Wei, Y. Zhuang, S. Liu, Q. Zhao, X. Zhang and W. Huang, *Adv. Optical Mater.*, 2017, **5**, 1700359; (e) Z.-P. Yan, K. Liao, H.-B. Han, J. Su, Y.-X. Zheng and J.-L. Zuo, *Chem. Commun.*, 2019, **55**, 8215; (f) J. Zhang, Q. Liu, W. Wu, J. Peng, H. Zhang, F. Song, B. He, X. Wang, H. H.-Y. Sung, M. Chen, B. S. Li, S. H. Liu, J. W. Y. Lam and B. Z. Tang, *ACS Nano*, 2019, **13**, 3618.
- 13 B. Wex and B. R. Kaafarani, *J. Mater. Chem. C*, 2017, **5**, 8622.
- 14 (a) K. Tani, R. Imafuku, K. Miyanaga, M. E. Masaki, H. Kato, K. Hori, K. Kubono, M. Taneda, T. Harada, K. Goto, F. Tani and T. Mori, *J. Phys. Chem. A*, 2020, **124**, 2057; (b) S. Kasemthaveechok, L. Abella, M. Jean, M. Cordier, T. Roisnel, N. Vanthuyne, T. Guizouarn, O. Cador, J. Autschbach, J. Crassous and L. Favereau, *J. Am. Chem. Soc.*, 2020, **142**, 20409; (c) M. Li, Y.-F. Wang, D. Zhang, L. Duan, C.-F. Chen, *Angew. Chem. Int. Ed.*, 2020, **59**, 3500; (d) Y.-F. Wang, M. Li, W.-L. Zhao, Y.-F. Shen, H.-Y. Lu, C.-F. Chen, *Chem. Commun.*, 2020, **56**, 9380; (e) G. Albano, L. A. Aronica, A. Minotto, F. Cacialli and L. Di Bari, *Chem. Eur. J.*, 2000, **26**, 16622; (f) R. Takishima, Y. Nishii and M. Miura, *Org. Lett.*, 2021, **23**, 1349; (g) P. Sumsalee, L. Abella, T. Roisnel, S. Lebrequier, G. Pieters, J. Autschbach, J. Crassous and L. Favereau, *J. Mater. Chem. C*, 2021, **9**, 11905; (h) J.-K. Li, X.-Y. Chen, Y.-L. Guo, X.-C. Wang, A. C.-H. Sue, X.-Y. Cao and X.-Y. Wang, *J. Am. Chem. Soc.*, 2021, **143**, 17958.
- 15 (a) P. Pandit, K. Yamamoto, T. Nakamura, K. Nishimura, Y. Kurashige, T. Yanai, G. Nakamura, S. Masaoka, K. Furukawa, Y. Yakiyama, M. Kawano and S. Higashibayashi, *Chem. Sci.*, 2015, **6**, 4160; (b) S. Mallick, S. Maddala, K. Kollimalayan and P. Venkatakrishnan, *J. Org. Chem.*, 2019, **84**, 73.
- 16 For both **BiCz-1** and **BiCz-2**, (S)-enantiomers were simulated as representatives.
- 17 (a) T. Mori, *Chem. Rev.*, 2021, **121**, 2373; (b) B. Doistau, J.-R. Jiménez and C. Pigué, *Front. Chem.*, 2020, **8**, 555; (c) H. Kubo, T. Hirose, T. Nakashima, T. Kawai, J. Hasegawa and K. Matsuda, *J. Phys. Chem. Lett.*, 2021, **12**, 686.